

RESEARCH ARTICLE

Lgd regulates the activity of the BMP/Dpp signalling pathway during *Drosophila* oogenesis

Kim Sara Morawa*, Markus Schneider* and Thomas Klein†

ABSTRACT

The tumour suppressor gene *lethal (2) giant discs (lgd)* is involved in endosomal trafficking of transmembrane proteins in *Drosophila*. Loss of function results in the ligand-independent activation of the Notch pathway in all imaginal disc cells and follicle cells. Analysis of *lgd* loss of function has largely been restricted to imaginal discs and suggests that no other signalling pathway is affected. The devotion of Lgd to the Notch pathway was puzzling given that *lgd* loss of function also affects trafficking of components of other signalling pathways, such as the Dpp (a *Drosophila* BMP) pathway. Moreover, Lgd physically interacts with Shrub, a fundamental component of the ESCRT trafficking machinery, whose loss of function results in the activation of several signalling pathways. Here, we show that during oogenesis *lgd* loss of function causes ectopic activation of the *Drosophila* BMP signalling pathway. This activation occurs in somatic follicle cells as well as in germline cells. The activation in germline cells causes an extra round of division, producing egg chambers with 32 instead of 16 cells. Moreover, more germline stem cells were formed. The *lgd* mutant cells are defective in endosomal trafficking, causing an accumulation of the type I Dpp receptor Thickveins in maturing endosomes, which probably causes activation of the pathway. Taken together, these results show that *lgd* loss of function causes various effects among tissues and can lead to the activation of signalling pathways other than Notch. They further show that there is a role for the endosomal pathway during oogenesis.

KEY WORDS: Cc2d1a, Aki, Tape, Dpp, Lgd [L(2)gd1], Notch signalling, Endocytosis

INTRODUCTION

In recent years, it has been established that the tumour suppressor gene *lethal (2) giant discs (lgd)* [l(2)gd1 – FlyBase] has a function in the endosomal pathway and in the regulation of the activity of the Notch pathway in *Drosophila melanogaster* (Childress et al., 2006; Gallagher and Knoblich, 2006; Jaekel and Klein, 2006; Schneider et al., 2013; Troost et al., 2012). Loss of its function leads to a defect in endosomal trafficking of transmembrane proteins, which accumulate in maturing endosomes (MEs). This defect causes the constitutive activation of the Notch pathway in a ligand-independent manner. *lgd* encodes a member of an evolutionary conserved family whose members contain four repeats of the novel DM14 domain followed by one C2 domain. A mutation in one of the two human orthologs, LGD2 (also named Aki, Freud-1, TAPE and Cc2d1a), causes mental retardation (Basel-Vanagaite et al.,

2006), and this protein might be a tumour suppressor in liver cells (Zender et al., 2008).

In *Drosophila* the Notch receptor is activated by two ligands, Delta (Dl) and Serrate (Ser) (reviewed by Bray, 2006). Their binding initiates the S2-cleavage of the extracellular domain of Notch (NECD). The cleaved NECD is then trans-endocytosed together with the ligand into the signal-sending cell. The cleavage is performed by a metalloproteinase encoded by *kuzbanian (kuz)* in *Drosophila*. The resulting intermediate Notch extracellular truncation (NEXT) fragment is cleaved by the γ -secretase complex, which contains Aph-1 and Presenilin (Psn). This S3-cleavage releases the Notch intracellular domain (NICD) into the cytosol from where it migrates into the nucleus to activate the target genes together with Suppressor of Hairless [Su(H)]. Previous work has shown that the constitutive activation of Notch observed in *lgd* mutant cells requires the activity of the γ -secretase complex (Jaekel and Klein, 2006).

Notch traffics constitutively through the endosomal pathway to be degraded in the lysosome (Jékely and Rørth, 2003). Trafficking is initiated by endocytosis, which results in the formation of early endosomal vesicles (reviewed by Huotari and Helenius, 2011). These vesicles fuse to form the early endosome (EE). Receptors destined for degradation remain in the ME, which eventually fuses with the lysosome where the cargo is degraded. During maturation of the endosome, receptors are concentrated in domains of its limiting membrane (LM) and are translocated into the lumen of the ME through pinching off this part as intraluminal vesicles (ILVs). The formation of ILVs achieves the separation of the NICDs of receptors from the cytosol. This step is important for the complete degradation of receptors as well as the termination of signalling through activated receptors.

The events in the endosomal pathway are controlled by small GTPases, chiefly Rab5 and Rab7 (Huotari and Helenius, 2011). Rab5 orchestrates events in the EEs, such as the initiation of ILV formation through recruitment of endosomal sorting complexes required for transport (ESCRT)-0, the first of five sequentially acting complexes, termed ESCRT-0–ESCRT-III and Vps4 (reviewed by Hurley, 2010). ESCRT-0 initiates the sequential recruitment of the complexes and concentrates ubiquitylated receptors in regions of ILV formation. ESCRT-0 consists of Hrs and Stam. The central component of the last acting ESCRT-III complex in *Drosophila* is encoded by *shrub*. It encodes the *Drosophila* ortholog of mammalian CHMP4 family proteins and yeast Snf7. Shrub is recruited to the LM of the MEs where it polymerises into filaments to perform the abscission of ILVs in concert with the Vps4 complex. As a result of the action of the ESCRT complexes, the ME contains an increasing number of ILVs and is called a multi-vesicular body (MVB). A recent paper provides evidence that suggests that LGD2 also interacts with CHMP4 during budding of HIV (Martinelli et al., 2012; Usami et al., 2012). Although the loss of the function of the ESCRT-I, -II and -III results

Institut für Genetik, Heinrich-Heine-Universität Düsseldorf, Universitätsstr. 1, Düsseldorf 40225, Germany.

*These authors contributed equally to this work

†Author for correspondence (thomas.klein@uni-duesseldorf.de)

in activation of the Notch and other signalling pathways in *Drosophila*, that of ESCRT-0 does not (Jaekel and Klein, 2006). An explanation for this puzzling fact is that ESCRT-0 performs an additional function that is required for activation in ESCRT-I, -II and -III mutants. This might consist of clustering of cargo at sites of ILV formation (Tognon et al., 2014). The additional function of ESCRT-0 is also required for the activation of the Notch pathway in *lgd* mutant cells because concomitant loss of ESCRT-0 and *Lgd* activity suppresses Notch activation (Gallagher and Knoblich, 2006; Jaekel and Klein, 2006).

We have recently shown that *Lgd* physically interacts with the ESCRT-III core component Shrub (Troost et al., 2012). This interaction is important for the full activity of Shrub *in vivo*. Genetic experiments have revealed that the activation of Notch in *lgd* mutant cells requires the Rab7-mediated fusion of the ME with the lysosome (Schneider et al., 2013). Furthermore, every other manipulation that prevents fusion of the ME with the lysosome, such as loss of Rab7 function, suppresses activation of Notch in *lgd* mutant cells (Schneider et al., 2013). This requirement for fusion explains a paradox in the relationship between *Lgd* and Shrub: the activation of Notch in *lgd* mutant discs is suppressed if the activity of *shrub* is reduced to 50%, although their individual loss results in Notch activation (Troost et al., 2012). The paradox could be explained by the observation that the MEs of these cells lose association with Rab7 and fail to fuse with the lysosome (Schneider et al., 2013). Thus, Notch pathway activation fails because the endosomes are more dysfunctional than in *lgd* mutant cells.

In *Drosophila*, loss of function of ESCRT-I, -II and -III in imaginal discs results in the ectopic activation of the Notch pathway. In addition, the activity of the *Drosophila* BMP pathway, called the Decapentaplegic (Dpp) pathway, is enhanced (Thompson et al., 2005; Vaccari and Bilder, 2005). Moreover, loss of ESCRT function causes loss of epithelial integrity (Thompson et al., 2005; Vaccari and Bilder, 2005). However, our previous analysis in imaginal discs indicates that neither the activity of other major signalling pathways, such as the Dpp pathway, nor the epithelial integrity is affected by the loss of *lgd* function (Schneider et al., 2013). Hence, the phenotype of ESCRT mutants is more severe than that of loss-of-function *lgd* mutants despite their intimate relationship.

The analysis of signalling pathways in *lgd* mutants described above was restricted to imaginal discs and indicated that only the Notch pathway is affected. It is not known whether these pathways are affected in other mutant tissues. The development of the oocyte of *Drosophila* is an excellent system to study cellular processes, such as cell signalling and, thus, to answer this question (reviewed by Bastock and St Johnston, 2008). During oogenesis the progenies of a germline stem cell (GSC) develops through distinct and recognisable stages into a mature egg in the ovariole. The ovariole is subdivided into an anterior germarium, which contains two kinds of stem cells and a posterior part that consists of a string of increasingly older egg chambers (ECs) with 16 germline cells (GCs) surrounded by a somatic follicle epithelium. The ECs bud off the germarium and mature upon their posterior migration. The GSCs are located at the anterior tip of the germarium and are surrounded by somatic cap cells, which form the niche required for their survival. The niche can accommodate 2–3 GSCs. These divide asymmetrically to give rise to another GSC and a cystoblast that begins to differentiate. The cystoblast undergoes four rounds of mitotic divisions to give rise to a cyst with 16 GCs. The cyst is encapsulated by somatic follicle cells (FCs) to generate the EC. The FCs are generated by two somatic stem cells located at the exit of the germarium. One GC in each EC

will differentiate into the oocyte, whereas the other 15 differentiate into polyploid nurse cells.

Several signals are required to maintain the GSC population. These are emitted at the tip of germarium by cap cells (Harris and Ashe, 2011). The most important one is Dpp. Although anterior cap cells are probably responsible for the majority of the Dpp signal, the extent of its expression domain remains unclear (Harris and Ashe, 2011). Dpp activates the co-receptor Thickveins (Tkv; type 1) and type 2 receptors on GSC (Xie and Spradling, 2000). The result of Dpp signalling is the suppression of the expression of *bag of marbles* (*bam*) in the GSC. When a GSC divides, the daughter attached to the cap cell receives the Dpp signal, which suppresses *bam* expression and maintains the GSC fate. The non-contacting daughter cell does not receive sufficient signal and produces Bam, which causes its differentiation as a cystoblast. Thus, Bam silencing is the hallmark of asymmetry in the female germline of *Drosophila*. The short range of the Dpp signal is achieved through degradation of the activated Tkv receptor in the cystoblast by a specific mechanism that involves the kinase Fused (Fu) and the E3 ligase Smurf (Xia et al., 2010). If the mechanism is disturbed, for example, by inactivation of *fu*, the number of GSCs increases and an extra round of division of the cyst cells occurs, frequently giving rise to ECs with 32 instead of 16 GCs (Narbonne-Reveau et al., 2006).

One well-characterised event during oogenesis that is mediated through the Notch signalling pathway is the switch from the mitotic cycle to the endocycle in FCs of ECs, which occurs at between stage 6 and 7 (Bastock and St Johnston, 2008). This switch is triggered by a DI signal from the GCs and initiates the differentiation of FCs through activation of Hindsight (Hnt) expression. We have shown that the loss of function of *lgd* in FCs results in precocious activation of the Notch pathway and expression of Hnt (Schneider et al., 2013). As in wing discs, the activation was independent of Kuz, and depended on Hrs and fusion of the ME with the lysosome (Schneider et al., 2013). Hence, the activation is caused by the same mechanism as in the wing disc.

The consequence of loss of *lgd* function in the germline was investigated previously using the allele *lgd^{Δ13}* (Szabad et al., 1991). The authors observed ECs with more than 40 GCs, a feature characteristic of tumour suppressor mutants. However, the analysis was hampered by the uncertain nature of *lgd^{Δ13}* and the lack of appropriate markers.

Here, we further investigated the function of *lgd* during oogenesis. We found that its loss causes activation of the Dpp pathway in addition to the Notch pathway in FCs. In the germline, loss of function of *lgd* causes an extra mitotic division that produces ECs with 32 GCs. In addition, it causes formation of more GSCs. Both phenotypes rely on ectopic activation of the Dpp. Our results indicate that these phenotypes are caused by a failure to degrade Tkv. Moreover, we found that the loss of function of *shrub* results in a similar phenotype.

RESULTS

In order to test whether other signalling pathways besides the Notch pathway are activated as a consequence of loss of *lgd* function during oogenesis, we monitored the activity of the Dpp pathway and compared it with that of the Notch pathway. In the following, we first describe the effects of loss of *lgd* function in FCs and then turn to the germline.

The Dpp pathway is activated in *lgd* mutant follicle cells

dad-lacZ has been extensively used to detect the activity of the Dpp pathway. During normal development expression of *dad-lacZ* is

restricted to the GSCs and initiated in FCs only from stage 9 onwards (Kai and Spradling, 2003) (Fig. 1C,D, arrow). In order to monitor the activity of the pathway in *lgd* mutant FCs, we induced *lgd* mutant clones and analysed the expression of *dad-lacZ*. We found that *dad-lacZ* is ectopically activated in all *lgd* FCs (Fig. 1E–H,M–P). Activation had already occurred by the time FCs of ECs had budded off the germarium (arrowhead in Fig. 1E–H). The activation is strictly cell-autonomous. We confirmed this finding using a *dad*-promoter-GFP construct (data not shown).

Given that loss of *lgd* results in activation of the Notch pathway, we tested whether *dad-lacZ* is a tissue-specific target of it. We therefore inactivated the pathway in *lgd* cells through inactivation of the γ -secretase component Aph-1 (Fig. 2A–H). Loss of *aph-1* function suppresses ectopic Notch signalling in *lgd* FCs (Schneider et al., 2013). By contrast, we found that *dad-lacZ* was still expressed in *lgd aph-1* clones, indicating that its expression in *lgd* FCs is independent of the activity of the Notch pathway (Fig. 2E–H, arrow).

We next inactivated the Dpp pathway in *lgd* FCs. As expected, no *dad-lacZ* expression was observed upon loss of *tkv* function alone (Fig. 2I–L, arrow). However, the ectopic expression of *dad-lacZ* was abolished in *lgd tkv* clones (Fig. 2M–P, arrow). Thus, ectopic activation of the Dpp pathway causes the observed ectopic expression of *dad-lacZ* in *lgd* cells and requires its receptor to do so. In contrast to *dad-lacZ*, Hnt was still precociously expressed in the *lgd tkv* FCs (Fig. 2Q–S, arrow). Given that Hnt is sufficient to drive the FCs into the endocycle, it is likely that the precocious switch to the endocycle observed in *lgd* mutants is unaffected by loss of Dpp signalling (Sun and Deng, 2007).

We have previously reported that the Dpp pathway is not ectopically activated in *lgd* mutant wing imaginal discs (Schneider et al., 2013). This conclusion was based on the analysis of other target genes. Here, we found that the expression of *dad-lacZ* was also unaffected by loss of *lgd* function in the wing disc (supplementary material Fig. S1A–D). Hence, activation of Dpp signalling is a tissue-specific response to loss of *lgd* function.

Activation of the Dpp pathway occurs in a different manner to that of the Notch pathway in *lgd* FCs

We were curious to test whether the activation of the Dpp pathway in *lgd* FCs depends on the function of *hrs* and occurs in the lysosome, as it is the case for the activation of the Notch pathway. However, expression of *dad-lacZ* was ectopically activated in *lgd hrs* FCs, indicating that the activation of the Dpp pathway is independent of the function of *hrs* (Fig. 3A–H, arrows). Dmon1 is required to recruit Rab7 to the endosome (Yousefian et al., 2013). The recruitment is necessary for the fusion of the ME with the lysosome. Hence, the MEs fail to fuse with the lysosome in *Dmon1* cells. In agreement with our previous findings, the ectopic activation of Notch signalling, measured with activity reporter Gbe+Su(H), was abolished in *lgd Dmon1* FCs and wing imaginal disc cells (Fig. 3L–P; supplementary material Fig. S1E,F). In contrast, *dad-lacZ* was expressed in *lgd Dmon1* FCs, indicating that the ectopic activation of the Dpp pathway does not require ME-lysosome fusion (Fig. 3I–O). Taken together, these results suggest that the activation of the Dpp pathway in FCs occurs in a different manner to that of the Notch pathway.

Note, that weak ectopic activation of *dad-lacZ* can also be observed in the *Dmon1/+ lgd/+* double heterozygous cells (Fig. 3I–K, red arrow). Moreover the activation of the reporter is stronger in *lgd Dmon1* cells than in *lgd* cells (Fig. 3I–O, compare with Fig. 1E–H). Given that the loss of *Dmon1* function does not result in activation of *dad-lacZ* expression, this finding indicates that the loss of *Dmon1* function enhances the ectopic activation of the Dpp pathway caused by loss of *lgd* function (Fig. 3I–P).

Loss of *lgd* function in GCs causes a defect in protein degradation

Next, we investigated the consequences of loss of function of *lgd* in the female germline using clonal analysis. We found that *lgd* GCs contained huge endosomes, which were positive for the endosomal markers Rab5 and Rab7, identifying them as MEs

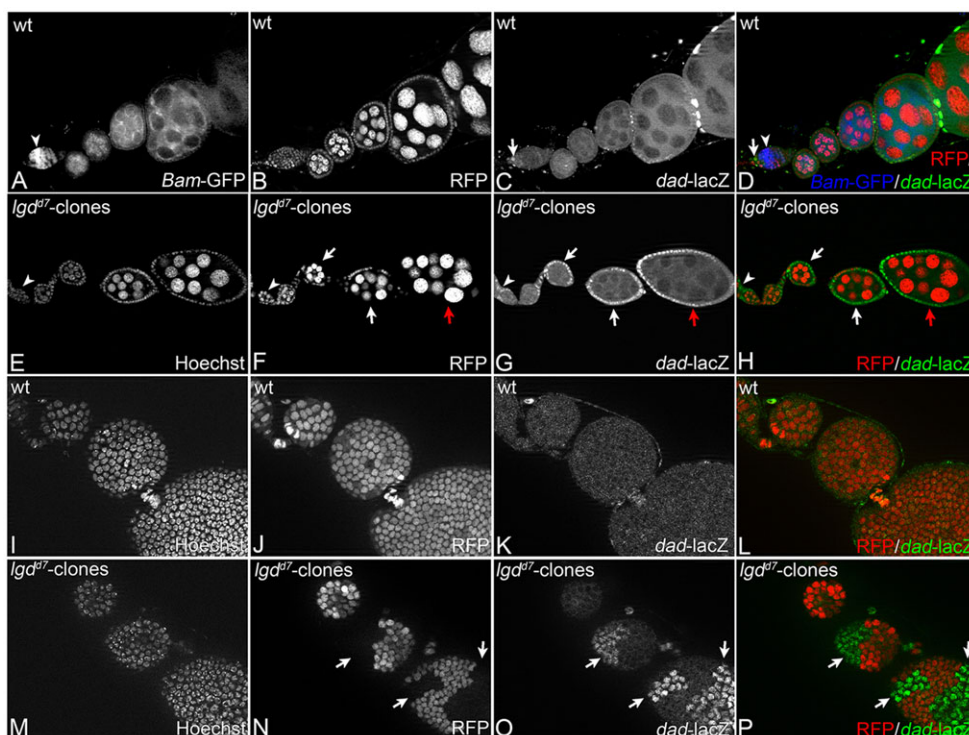


Fig. 1. Loss of *lgd* function results in ectopic activation of expression of *dad-lacZ* in FCs. (A–D) Overview of expression of *dad-lacZ* and *Bam-GFP* in a wild-type (wt) ovariole. Expression of *dad-lacZ* occurs in the two GSCs in the germarium (arrow). *Bam-GFP* is expressed in cystoblasts and upregulated during the mitotic cyst stages in the germarium (arrowhead). (E–H) An ovariole where most of the FCs are mutant for *lgd*, indicated by the loss of RFP. These FCs activate expression of *dad-lacZ* (arrows). The red arrow highlights an older stage EC (stage 8/9) with *lgd* mutant FC; the expression of *dad-lacZ* is still maintained. The arrowhead points to mutant *dad-lacZ*-positive FCs at the exit of the germarium. (I–L) Magnification of egg chambers of the wild-type ovariole shown in A–D. The focus is on the FCs, which do not express *dad-lacZ*. (M–P) Magnification of egg chambers of the ovariole with *lgd* mutant clones shown in E–H. The mutant FCs (labelled by loss of RFP) express *dad-lacZ* (arrows).

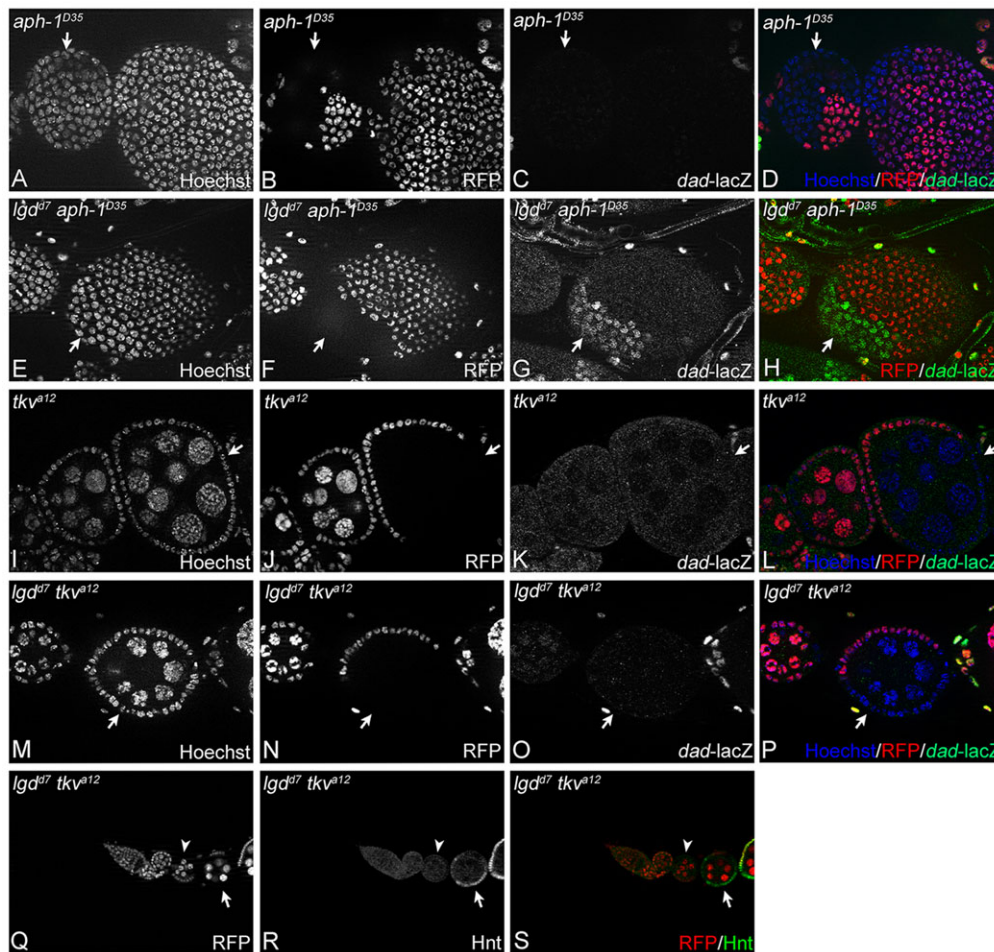


Fig. 2. Activation of *dad-lacZ* expression in *lgd* FCs is caused by the ectopic activation of the Dpp pathway. Clones are labelled by absence of RFP. (A–D) *aph-1* clones (arrow). (E–H) *aph-1 lgd* clones (arrow). (I–L) *tkv* clones (arrow). (M–P) *tkv lgd* clones lose *dad-lacZ* expression (arrow). (Q–S) Hnt expression in *lgd tkv* cell clones of stage 6 egg chambers (arrow). The arrowhead highlights a double-mutant EC in early stages where Hnt is not expressed due to only weak ectopic activation of the Notch pathway, which is insufficient for activation of Hnt (Schneider et al., 2013).

(Fig. 4A–J, arrowheads). The enlargement of MEs was also previously observed in *lgd* mutant FCs and indicates a defect in endosome maturation (Schneider et al., 2013). Using the Gbe+ Su(H) reporter, we fail to observe activation of the Notch pathway in *lgd* GCs (data not shown). Thus, we were surprised to observe the NECD in mutant MEs (Fig. 4A–J). The NECD could stem from the GCs, which weakly express Notch. In this case, one would also expect to detect the NICD. Alternatively, the NECD in MEs could be the consequence of transendocytosis, which occurs during DI signalling from GCs to FCs (Parks et al., 2000). In this case, NICD should be absent from GCs. To investigate the origin of NECD, we used a gene trap in *Notch*, which encodes a functional variant with YFP inserted in the NECD (YFP-Notch) (Rees et al., 2011). We used YFP-Notch in combination with an antibody directed against NICD to detect both parts of the receptor. In *lgd* GCs we detected the YFP-NECD, but not the NICD (Fig. 4N–Q). Thus, the GCs appear to take up NECD from the surrounding Notch-expressing FCs. In agreement with this conclusion, we found that DI localises with NECD in the MEs of *lgd* GCs (supplementary material Fig. S2A–J). Moreover, we found that *DI lgd* GCs failed to incorporate NECD, whereas *lgd* GCs in other ECs of the same ovariole did so (supplementary material Fig. S2K–N). This result confirms that the incorporation of NECD is a consequence of signalling from GCs to FCs. Given that accumulation of NECD is hardly seen in wild-type GCs, it is likely that the *lgd* GCs are defective in degradation of DI-NECD and other transmembrane proteins. The defect reveals the trans-endocytosis event during Notch signalling in an unprecedented clarity.

Loss of *lgd* function in the germline results in formation of additional GCs

In order to confirm that loss of function of *lgd* results in the formation of supernumerary GCs, we analysed *lgd*-null mutant germline clones. *lgd^{d7}* is a null allele that fails to produce detectable levels of proteins (Childress et al., 2006; Jaekel and Klein, 2006). In agreement with the report of Szabad et al. (1991), we found that a fraction of ECs with an *lgd^{d7}* mutant germline contained supernumerary GCs (Fig. 5A–L). Quantification of this phenotype revealed that it occurs in 15% of the analysed ECs (Fig. 6; $n=500$). These ECs contained exactly twice as much GCs as normal ones (32 cells; see supplementary material Movie 1). The nuclei of these GCs are smaller than that of normal GCs, indicating a lower degree of endoreplication (compare Fig. 5H with K, arrowhead). We observed the same phenotype using the independently induced null allele *lgd^{trsk73a}* (Fig. 6). Moreover, the phenotype was rescued by the presence of two copies of an *lgd-RFP* rescue construct (Troost et al., 2012) (Fig. 6). Thus, the 32 GCs phenotype is caused by the loss of *lgd* function.

ECs with 32 GCs could result from fusion of two normal ECs or from an additional round of division of the GCs. The two possibilities can be discriminated by determining the number of oocytes: if fusion occurs, two oocytes would be present in the EC, whereas one would be present if an extra round of division occurs. Orb is a specific oocyte marker. Only one Orb-positive GC was present in ECs with 32 GCs (Fig. 5M–O). Moreover, YFP-Tkv accumulates in the oocyte and can be therefore used as a marker (see below). In ECs with 32 cells, only one cell accumulated YFP-Tkv

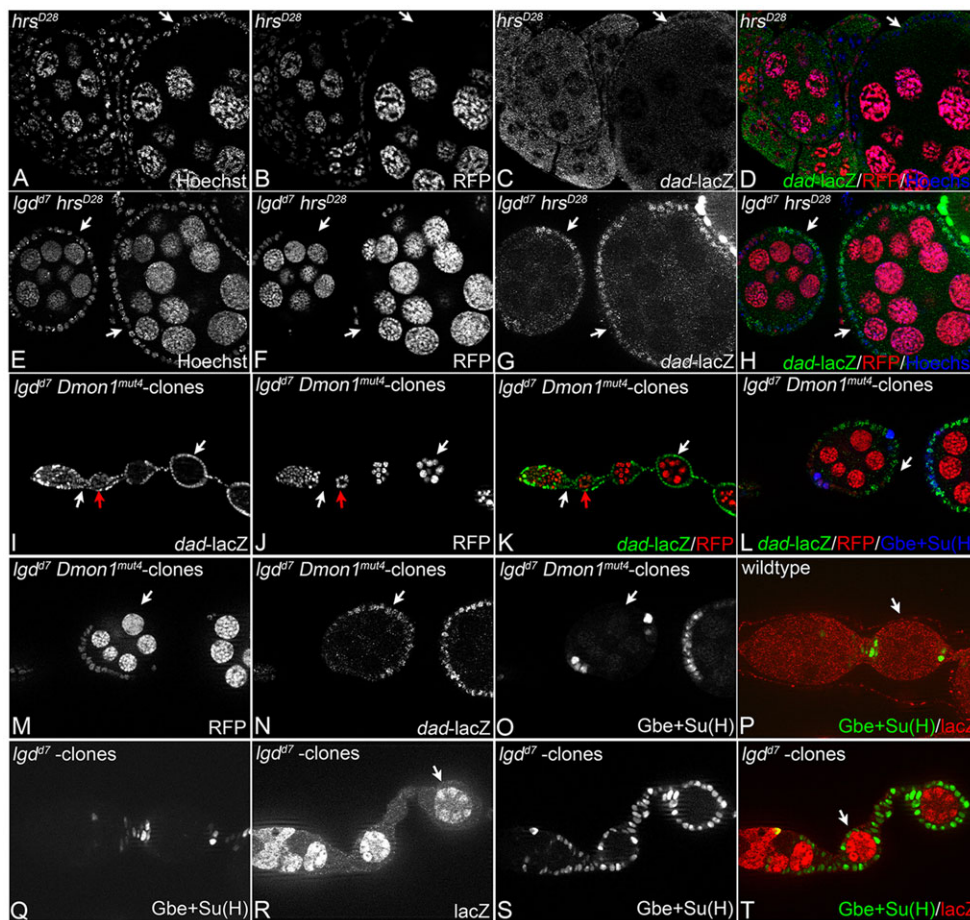


Fig. 3. The activation of the Dpp pathway occurs by another mechanism than through the Notch pathway. The white arrows point to the clones in the follicle epithelium. (A–D) Expression of *dad-lacZ* in *hrs* clones. (E–H) *dad-lacZ* expression in *hrs lgd* FC clones. (I–O) Expression of *dad-lacZ* and Gbe+Su(H)-GFP in *Dmon1 lgd* clones. (P) Expression of Gbe+Su(H)-GFP in wild-type FCs. (Q–T) Expression of Gbe+Su(H)-GFP in *lgd* clones.

(Fig. 5P–R, arrowhead). The oocyte is the only cell in the egg chamber that maintains its diploid state. Its nucleus is therefore smaller than that of the polyploid nurse cells. Only one small nucleus was present at the posterior end of *lgd* ECs with 32 FCs (Fig. 5K, arrow). Thus, it appears that the 32 GC phenotype is caused by an additional round of division.

We tested whether we could detect an additional round of division in *lgd* mutant germaria using the mitotic marker Cyclin A (CycA, Fig. 5S–X). CycA is expressed in early, but not older posterior cysts (Fig. 5S–U, arrowhead). We observed a fraction of *lgd* germaria (14%, $n=21$) where all cysts express CycA (Fig. 5V–X, arrowhead). The frequency is similar to that of EC with 32 cells (Fig. 6). This finding further supports our notion that a fraction of *lgd* cysts undergo an extra round of mitotic division.

Loss of *lgd* function in GCs results in activation of the Dpp pathway

The 32 GC phenotype is not caused by ectopic activation of the Notch pathway, as it is also observed in *lgd aph-1* germline clones (Fig. 6). Thus, we asked whether ectopic activation of the Dpp pathway occurs in *lgd* GCs. Indeed, we observed ectopic expression of *dad-lacZ* in *lgd* GCs (Fig. 7A,B, compare with Fig. 1A–D). The expression is initiated in cysts at the exit of the germarium (region 2b, white arrow in Fig. 7A,B), peaked at stage 2 (red arrow) and continued in ECs until stage 6 (arrowhead). It was abolished in *lgd tkv* GCs (Fig. 7C–E). Taken together, these results indicate that the Dpp pathway is ectopically activated in GCs upon loss of *lgd* function at a time consistent with a role in induction of an extra round of cell division.

Ectopic activation of the Dpp pathway causes the formation of ECs containing 32 GCs

Next, we tested whether the ectopic activation of the Dpp pathway is required for the formation of supernumerary GCs upon loss of *lgd* function. Therefore, we monitored *lgd tkv* germline clones and failed to detect ECs with 32 GCs in this situation (Fig. 6). Thus, ectopic Dpp signalling is required for the extra round of division of *lgd* GCs. Ectopic activation of *dad-lacZ* in *lgd* GCs was observed irrespective of whether the ECs contained 16 or 32 cells (Fig. 7B, red and yellow arrows). Hence, activation of the Dpp pathway is required, but is not sufficient, for the extra round of cell division of mutant germaries. Alternatively, the levels of Dpp signalling might fluctuate around threshold levels required for extra division.

The main function of Dpp signalling in the germarium is to suppress expression of Bam in GSCs (Bastock and St Johnston, 2008). Consequently, expression of Bam is initiated in cystoblasts and strongly upregulated during mitotic cyst stages in the germarium (Fig. 7F–H, wt). We found that expression of Bam-GFP was altered in many *lgd* mutant germaria. In some cases the Bam-GFP expression was suppressed, whereas in other cases no obvious changes were observed (Fig. 7F–L). Nevertheless, expression of high Bam and *dad-lacZ* were mutually exclusive. Moreover, in germaria with high Bam-GFP expression, *dad-lacZ* reappeared in older *lgd* cysts with no expression of Bam (yellow arrow in Fig. 7I–L). These findings reconfirm that Dpp is activated and suggest that its activity fluctuates around the threshold level required to suppress the expression of Bam.

During this analysis, we observed more *dad-lacZ*-positive cells at the tip of the germarium where the GSCs are located (Fig. 7J,L,

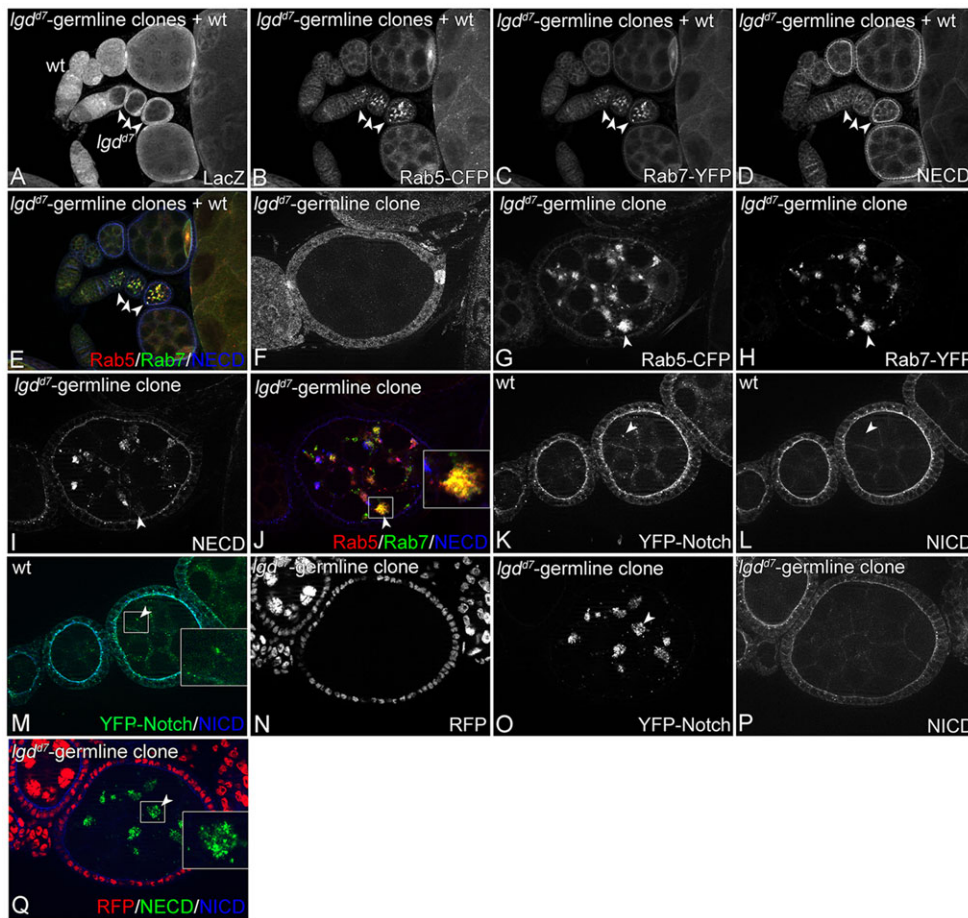


Fig. 4. Loss of *Igd* function in the germline causes an endosomal degradation defect. (A–E) An ovariole bearing *Igd* germline clones next to a wild-type (wt) ovariole. The mutant GCs have endosomes that are positive for NECD, Rab5 and Rab7 (arrowheads). (F–J) Magnification of an EC with a mutant germline, shown at higher magnification. The arrowhead points to an enlarged ME. (K–M) Expression of YFP-Notch in comparison to NICD. The arrowhead points to the YFP-Notch-positive endosomes of GCs. NICD is absent. (N–Q) Egg chamber with *Igd* GCs. YFP-Notch accumulates at high levels in the enlarged endosomes of mutant GCs (arrowhead). NICD is absent.

arrow). These cells were Bam negative, indicating that they are GSCs. Counting revealed that *Igd* germaria contained one additional GSC (Fig. 8), suggesting an increase of the range of the Dpp signal.

The Tkv receptor accumulates in MEs of *Igd* cells

The above data indicate that ectopic activation of the Dpp pathway in *Igd* mutant GCs is dependent on Tkv and show that the cells are defective in degradation of transmembrane proteins. Thus, we asked whether the degradation of Tkv is defective in *Igd* mutant GCs. In order to monitor the expression of Tkv, we used a gene trap where YFP is inserted in the N-terminus of Tkv (YFP-Tkv) (Kyoto Stock Center). This variant is fully functional. Given that expression of Tkv during oogenesis has not been described, we provide a detailed description in supplementary material Fig. S3. In short, Tkv is expressed in all cells of the germarium at different levels during normal oogenesis. The loss of *Igd* function results in a strong accumulation of YFP-Tkv in the NECD-positive enlarged vesicles of GCs (Fig. 9A–H, arrowheads in F–H). The majority of these vesicles were Rab7 positive, identifying them as MEs (Fig. 9I–L). We found a similar accumulation in Notch-positive MEs of *Igd* mutant FCs (Fig. 9M–P, arrow). Taken together, the results suggest that the degradation defect also causes the accumulation of Tkv in mutant MEs.

To find further evidence that the degradation defect causes ectopic activation of the Dpp pathway, we prevented degradation in the lysosome completely. Loss of *Dmon1* function prevents fusion of the ME with the lysosome (Yousefian et al., 2013). Hence, the lifetime of MEs is dramatically increased and degradation of cargo prevented. We found that loss of *Dmon1* function in the germline fails to activate

the Dpp pathway (supplementary material Fig. S4A–D). However, concomitant loss of *Dmon1* and *Igd* function resulted in enhanced activation of the Dpp pathway, which manifests itself through expression of *dad-lacZ* in most GCs of the germarium (Fig. 9Q–T). Moreover, we observed that all GCs in the germarium contained a spectrosome, which is a hallmark of GSCs (Fig. 9Q–T, arrowheads in S,T). This tumorous germarium phenotype is also observed upon ectopic activation of the Dpp pathway (Xie and Spradling, 2000). We also observed weak *dad-lacZ* expression in double heterozygous *Dmon1* and *Igd* mutant FCs, indicating that further delaying the degradation of Tkv in *Igd* GCs increases the activation of the Dpp pathway (arrow in Fig. 9Q–T). Given that loss of *Dmon1* function alone does not activate the pathway, the *Igd* mutant cells must have an additional defect in trafficking of Tkv that is required for the activation of the pathway besides delaying degradation.

Loss of function *shrub* causes activation of the Dpp pathway

Igd is required for the full function of *Shrub* (Troost et al., 2012). Moreover, loss of *shrub* function causes also ectopic activation of the Notch pathway in FCs (Vaccari et al., 2009). Therefore, we were curious whether the loss of *shrub* function causes the activation of the Dpp pathway during oogenesis. We found that *dad-lacZ* was also activated ectopically and cell-autonomously in *shrub* FC clones, suggesting that the Dpp pathway is activated (Fig. 10A,B).

shrub germline clones survived poorly and could not be analysed properly. However, we found that the reduction of *shrub* function by 50%, achieved through heterozygosity of a null allele (*shrub*^{4-1/+}), caused ectopic activation of *dad-lacZ* (Fig. 10C,D). Furthermore, we observed that 30% of the ECs contained 32 GCs (Fig. 6). Hence,

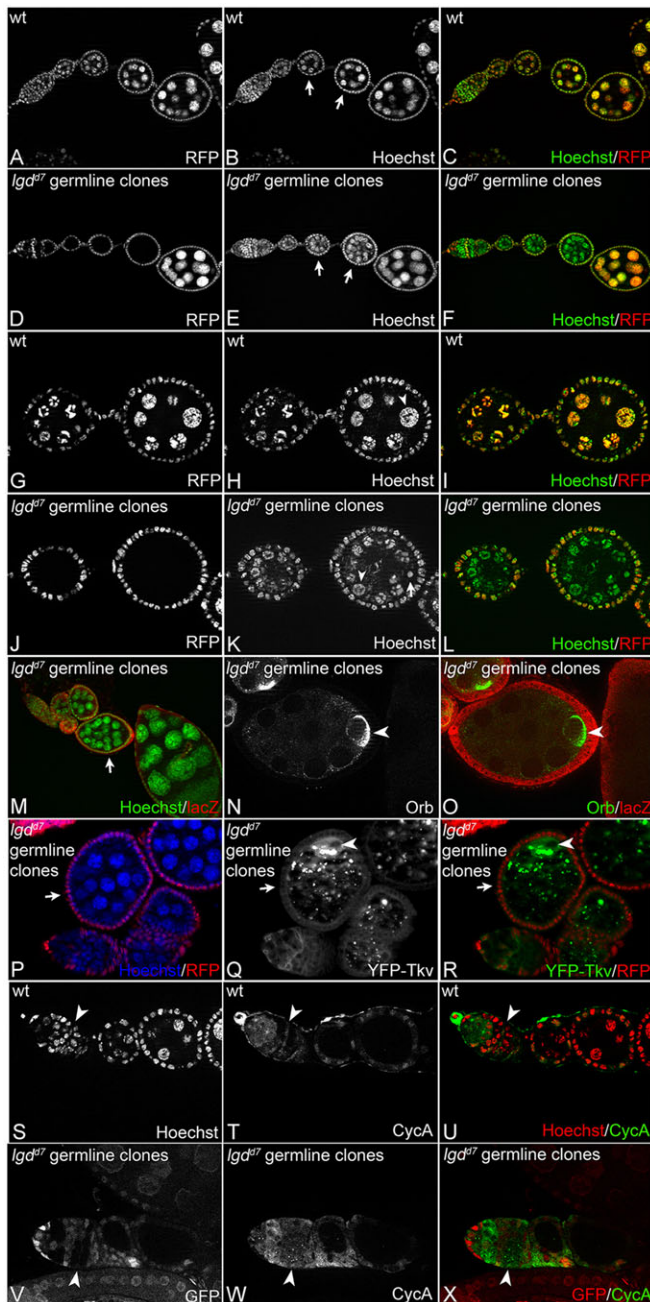


Fig. 5. *Lgd* mutant cysts undergo an extra mitotic division. (A–C) Wild-type (wt) ovariole. (D–F) A comparable ovariole bearing *lgd* germline clones. The arrows highlight two ECs with 32 GCs. (G–L) Magnification of the ECs highlighted with the arrows in B and E. The nuclei of mutant GCs are smaller (arrowhead in H,K). The arrow in (K) points to the small oocyte nucleus. (M) A mutant EC with 32 GCs (arrow). (N,O) A magnification of the EC highlighted with the arrow in M. One Orb-positive oocyte is present (arrowhead). (P–R) YFP-Tkv expression in an *lgd* EC with 32 GCs (arrow). One cell accumulates Tkiv (arrowhead). (S–X) Expression of CycA in wt and *lgd* ovarioles. The arrowhead points to late cyst stages which are devoid of CycA expression in the wild type (S–U). In a fraction of *lgd* ovarioles the expression is maintained in old cyst stages (arrowhead in V–X).

the reduction of *shrub* activity in GCs causes defects similar to that of loss of *lgd* function.

We further found that the *shrub*^{+/+} germaria contained more *dad-lacZ* GSCs than the wild-type, indicating that the range of the Dpp signal had increased (4.9 cells versus 2.6 cells; Fig. 8 and

Fig. 10C–F, arrowhead). Likewise, expression of Bam-GFP varied in *shrub*^{+/+} germaria. We found clearly abnormal expression of Bam-GFP in some germaria, where some of the cells in the Bam-GFP domain still expressed *dad-lacZ* but not Bam-GFP (Fig. 10E,F, arrows). In contrast the expression was close to normal in other germaria (Fig. 10C,D).

Despite the similarity in phenotype of *lgd* and *shrub* mutants, the fraction of egg chambers with 32 GCs decreased from 30% to 7% in *shrub lgd* double heterozygous flies (*shrub lgd*^{+/+}; Fig. 6). This suggests that the two genes have an antagonistic relationship. However, the double heterozygous germaria exhibited abnormal Bam-GFP expression and contained as many additional *dad-lacZ*-positive GSCs as described for *shrub* heterozygous flies (Fig. 10G,H, arrows and arrowheads, Fig. 8).

Functional interactions with *Fu* during germline development

The phenotype of *lgd* in the germline resembles that of *fu* mutants (Narbonne-Reveau et al., 2006). Therefore, we tested whether *lgd* and *shrub* have a functional relationship with *fu*. Indeed, we found that this is the case: loss of one copy of *fu* increased the number of GSCs by two (4.5), whereas loss of *lgd* function results in an increase by one (3.6; Fig. 8). However, the loss of one copy of *fu* in an *lgd* mutant germline increased the number of GSCs to 7 (Fig. 8). This suggests a further increase in the effective range of the Dpp pathway. Surprisingly, we detected a decrease in the number of ECs with 32 GCs in this genotype instead of the expected increase (Fig. 6). Nevertheless, both results indicate an existing functional relationship between both loci that might be more complicated than anticipated.

Similarly, loss of one copy of *fu* also enhanced the *shrub* heterozygous phenotype in the germline: the number of GSCs increased from 4.9 (*shrub*^{+/+}) to 6.7 (*fu*^{+/+}; *shrub*^{+/+}; Fig. 8). Moreover, the percentage of ECs containing 32 GCs increased from 29% (*shrub*^{+/+}) to 52% in *fu*^{+/+}; *shrub*^{+/+} animals (Fig. 8). Note, that the loss of one copy of *fu* alone failed to produce egg chambers with 32 GCs. These findings reveal a strong synergistic functional relationship between *shrub* and *fu*.

DISCUSSION

The previously conducted analysis of the function of *lgd* was largely restricted to imaginal discs. It suggested that loss of *lgd* function specifically activates the Notch pathway. Moreover, we showed that the loss of *lgd* function in FCs results in activation of the Notch pathway in the same manner as in imaginal disc cells. The deviation of Lgd to the Notch pathway was puzzling, given that it also controls trafficking of components of several signalling pathways, such as Tkiv (Jaekel and Klein, 2006). Lgd functionally interacts with Shrub, whose loss of function affects several signalling pathways in imaginal disc cells. Thus, it would be conceivable that these pathways are also activated in *lgd* mutant cells. Here, we show that the Dpp pathway is ectopically activated upon loss of function of *lgd* in the ovary. This activation occurs in FCs as well as GCs. Only the Dpp, and not the Notch, pathway is activated in *lgd* mutant GCs. Our observation is different from what has been reported for mutants of the ESCRT-II component Vps25, where Dpp signalling was enhanced, but the pathway not ectopically activated (Thompson et al., 2005).

We failed to detect any phenotype that could be attributed to the observed ectopic activation of the Dpp pathway in *lgd* mutant FCs, but found that its ectopic activation in the mutant germline causes an extra round of cell division. Moreover, more GSCs were observed and

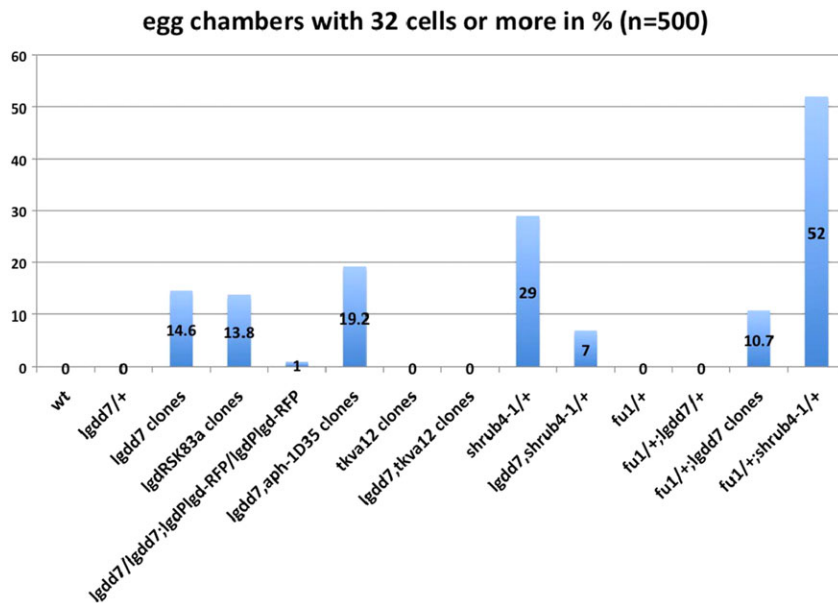


Fig. 6. Frequency of egg chambers with 32 GCs in various genotypes.

expression of Bam-GFP was suppressed in a fraction of germaria. These findings suggest that the range of the Dpp signal is extended and, thus, maintains the GSC fate in more distantly located cells.

It has been recently shown that the Dpp-activated form of the Tkv receptor is specifically degraded in cyst cells to suppress the ectopic activation of the pathway (Xia et al., 2010). This degradation through the endosomal pathway is mediated by a complex consisting of the E3 ligase Smurf and Fu, and restricts the activity of the pathway to GSCs in the cap cell niche. The loss of *fu* function causes a loss of degradation of the activated receptor in progenies of the GSCs and, thus, increases the range of the pathway in GCs. Hence, ectopic activation occurs cell autonomously, but is induced

by the Dpp ligand. The ectopic activity induced by loss of *fu* function causes a variety of phenotypes, including egg chambers that contain 32 GCs, as we have observed upon loss of *lgd* function here (Narbonne-Reveau et al., 2006). We have previously shown that loss of function of *lgd* results in a defect in the degradation of Tkv and other cargo proteins, such as Notch and D1, in FCs and GCs (Jaekel and Klein, 2006). We also found that the range of the Dpp pathway is increased in the absence of *lgd* function. It is therefore likely that the activation of the pathway is caused by a general failure of degradation that also affects the degradation of the activated form of Tkv. In further support of this notion, we discovered genetic interactions between *fu*, *lgd* and *shrub*.

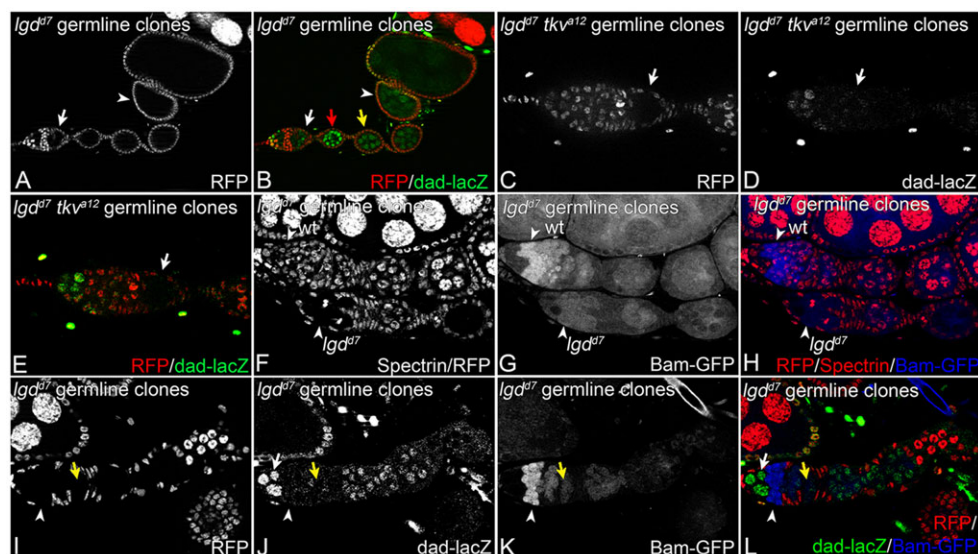


Fig. 7. Loss of *lgd* function in GCs results in activation of Dpp signalling. (A,B) An ovariole with an *lgd* germline (RFP negative). Expression of *dad-lacZ* is activated in GCs up to stage 6 (arrowhead). The white arrow highlights an egg chamber that emerges from the germarium and expresses *dad-lacZ*. The red arrow highlights a stage 2 EC where the *dad-lacZ* expression peaks. This EC contains 32 GCs. The yellow arrow highlights an EC with 16 GCs. (C,E) A stage 2 EC with a *lgd* *tkv* germline (arrow). (F–H) A wild-type (wt) germarium next to one with an *lgd* germline (RFP negative). Expression of Bam-GFP is upregulated in the mitotic cyst stages in the wild type, whereas it is strongly reduced in the mutant germarium (arrowheads). (I–L) A germarium with an *lgd* germline where the expression of Bam-GFP is unaffected and the upregulation of expression in mitotic cyst stages is clearly recognisable (arrowhead, compare with the wild-type germarium in F–H). Note, that the mutant germarium contains four *dad-lacZ*-expressing Bam-GFP-negative GSCs (arrow in J,L). The yellow arrow points to a single GC of an abutting egg chamber that expresses *dad-lacZ*.

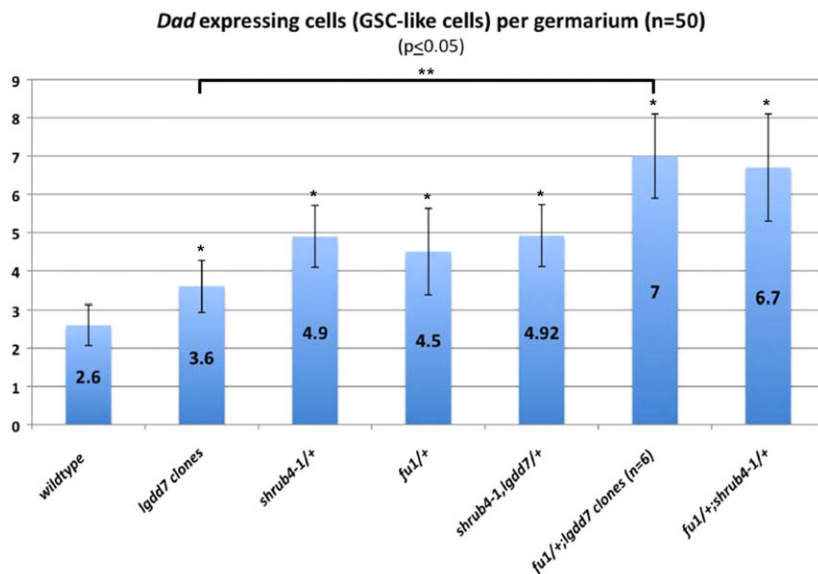


Fig. 8. Number of GSCs in wt, *lgd* mutant and *shrub* and *fu* heterozygous germlines. * $P < 0.05$, compared with wt; ** $P < 0.05$, *lgd* compared with *fu1/+;lgd*; t-test, normal distribution.

We have proposed that in *lgd* cells, transmembrane proteins destined to become degraded in the lysosome are not completely incorporated in ILVs of MEs (Schneider et al., 2013). This hypothesis has been strongly supported by recent work of the Schweisguth laboratory (Couturier et al., 2014). Consequently, a fraction of Notch and Tkv remains at the LM and their intracellular domains stay in contact with the cytosol. Activated Tkv in this fraction continues to signal as long as the ME exists. We therefore propose that it is the defect in

incorporation of activated Tkv into ILVs that causes the ectopic activation of the Dpp pathway. In this scenario, defects that increase the lifetime of the *lgd* mutant ME, such as loss of *Dmon1* function, enhances and prolongs the activity of the Dpp pathway. This is what we have observed. The incorporation of transmembrane proteins into ILVs requires their previous ubiquitylation by E3 ligases. Hence, the loss of the function of the E3 ligase Fu, which normally ubiquitylates activated Tkv, also prevents incorporation of activated Tkv in ILVs.

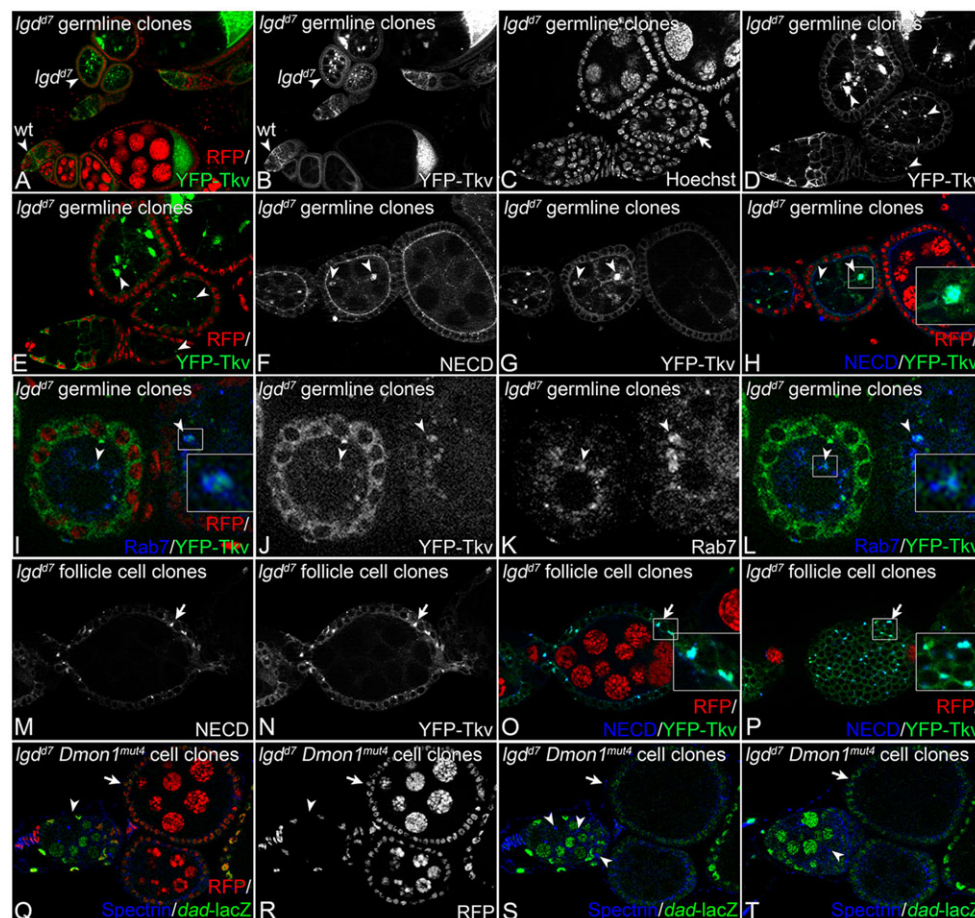


Fig. 9. Loss of *lgd* function causes accumulation of YFP-Tkv in FCs and GCs. Clones are labelled by the absence of RFP. (A,B) A wild-type (wt) ovariole next to an ovariole with *lgd* mutant GCs. The mutant GCs contain enlarged YFP-Tkv-positive vesicles (arrowhead). (C-E) Magnification of the mutant ECs highlighted in A,B with an arrowhead. (F-H) EC with an *lgd* mutant germline. The Tkv-containing vesicles also contain NECD (arrowheads). (I-L) The enlarged vesicles are positive for Rab7. (M-P) Accumulation of YFP-Tkv in endosomes of *lgd* FCs. (P) Surface view on the egg chamber shown in M-O. (Q-T) A germarium with an *lgd Dmon1* mutant germline (arrowhead). Different optical planes of the germarium shown in Q and R. The arrowheads point to the spectroscopes. The arrow in Q-T points to the double heterozygous FCs that weakly express *dad-lacZ*.

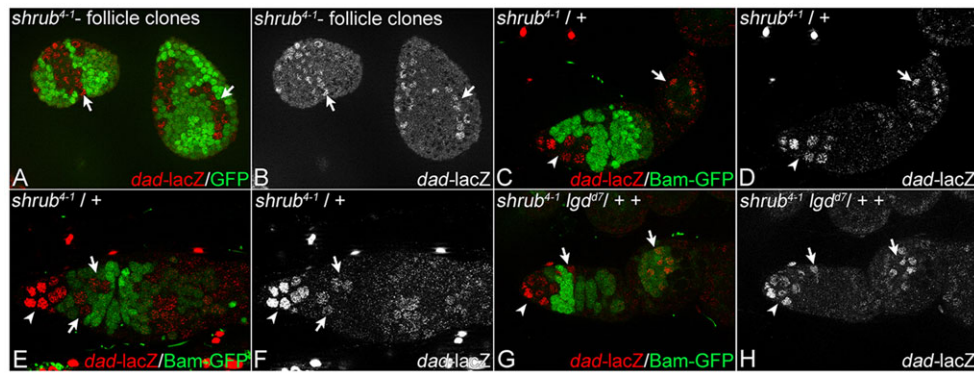


Fig. 10. Loss of *shrub* function causes ectopic activation of the Dpp pathway. (A,B) *dad-lacZ* expression in *shrub* FC clones (arrows) in two adjacent ECs. (C–E) Ectopic activation of *dad-lacZ* in *shrub*^{+/+} heterozygous GCs. The expression of Bam-GFP is close to normal. The arrow in C,D points to an EC with ectopic expression of *dad-lacZ* in the GCs. The arrow in E,F points to cysts with cells that have ectopically activated *dad-lacZ* and have already switched off Bam-GFP in the germarium. Note, the expression of *dad-lacZ* in more than the usual 2–3 GSCs in the anterior tip of the germaria (arrowheads in C–F). (G,H) *lgd shrub* double heterozygous ovariole. Ectopic *dad-lacZ* expression is still observed in cyst in the germaria and early egg chambers (arrows). The arrowhead points to the *dad-lacZ*-positive GSCs.

We found that loss of *shrub* function causes a similar defect to that of *lgd*. *Shrub* is the central element of the ESCRT-III complex, which is required for ILV scission and interacts physically with Lgd (Troost et al., 2012). Loss of *shrub* function is expected to result in all Tkv remaining on the LM. Thus, it was no surprise to see that loss of its function in the FCs also causes the activation of the Dpp pathway. More surprising was the finding that reduction of *Shrub* activity by only 50% is sufficient to initiate the activation of the Dpp pathway in the germline. Given that that phenotypes of *shrub*^{+/+} cells are stronger than those of *lgd* mutant cells, it is likely that reduction of the activity of *shrub* by 50% causes a larger fraction of Tkv to remain on the LM than in *lgd* mutant cells. The phenotypes of *shrub*^{+/+} cells are strongly enhanced by heterozygosity of *fu*, indicating that there is an intimate functional relationship and that, as in the case of *lgd*, a defect in Tkv degradation causes the activation of the Dpp pathway.

Because of the similarity in the phenotype and their intimate relationship, it is puzzling to find an antagonistic relationship between *shrub* and *lgd*. However, we observed this antagonism only in respect to the formation of supernumerary GCs, but not in respect to formation of supernumerary *dad-lacZ*-positive GSCs. A similar complex situation was found for the relationship of *shrub* and *lgd* in imaginal discs, where the reduction of *shrub* activity suppressed the activation of the Notch pathway, but enhanced the morphological defect of endosomes in *lgd* cells (Troost et al., 2012). Finding explanation for this complex relationship will be key to understanding the function of Lgd. One possibility is that the function of the ME is disturbed more severely in the double mutants than in each single mutant. In agreement with this is our observation in the imaginal disc, where the MEs lost their association with Rab7 in *shrub lgd/lgd*⁺ cells (Schneider et al., 2013).

MATERIALS AND METHODS

Drosophila genetics

The fly stocks used were as follows: tub *rab5*-CFP tub *rab7*-YFP (Marois et al., 2006), *Gbe+Su(H)*-nlsGFP (de Navascués et al., 2012), *bam*-GFP (kindly provided by Masahiko Takemura, Department of Biology, Graduate School of Science, Kobe, Japan), *N*-YFP (Rees et al., 2011), *dad-lacZ* (Casanueva and Ferguson, 2004) and *lgdP-lgd*-RFP (Troost et al., 2012). Mutant stocks were as follows: *shrub*⁴⁻¹ FRTG13 (Sweeney et al., 2006), *lgd*^{dl7} *aph-1*^{D35} FRT40A (Schneider et al., 2013), *hrs*^{D28} FRT40A (Lloyd

et al., 2002), *tkv*^{a12} FRT40A (Terracol and Lengyel, 1994), *lgd*^{dl7} *tkv*^{a12} FRT40A (this study), *aph-1*^{D35} FRT40A (Hu et al., 2002), *Dl*^{rev10} FRT82B (Micchelli et al., 1997), *lgd*^{dl7} FRT40A, *lgd*^{rsk73a} FRT40A and *lgd*^{dl7} *hrs*^{D28} FRT40A (Jaekel and Klein, 2006), *Dmon1*^{mut4} FRT40A (Yousefian et al., 2013), *lgd*^{dl7} *Dmon1*^{mut4} FRT40A (this study), *lgd*^{dl7} *tkv*-YFP FRT40A (this study), *fu*¹ (Nüsslein-Volhard and Wieschaus, 1980) and *lgd*^{dl7} *shrub*⁴⁻¹ FRT40A (Nadja Ohlenhard, diploma thesis, Heinrich-Heine-Universität, Düsseldorf). Other lines were: Tkv-YFP (Kyoto Stock Center), *dad*-GFP (Ninov et al., 2010) and *PCNA*-GFP (Thacker et al., 2003).

Clonal analysis

Follicle cell clones were generated with the Flp/FRT system (Xu and Rubin, 1993) and induced in adult females by applying a 2-h heat shock (37°C) on two consecutive days. Flies were kept at 25°C and ovaries were dissected 2 days after heat shock. Germline clones were induced in the first-instar larvae (24–48 h after egg laying) by applying a 90-min heat shock (37°C). Larvae were kept at 25°C and ovaries were dissected 2 days after eclosion.

Immunostaining and microscopy

Antibody staining was performed according to standard protocols. Ovaries were additionally stained with the nuclear marker Hoechst 33258. Antibodies used were: the mouse anti-Notch antibody against the extracellular domain (C458.2H), mouse anti-Notch antibody against the intracellular domain, and anti-Dl, anti-Orb, anti-CycA and anti-Hnt antibodies (169) (all obtained from DSHB Iowa). Further antibodies used in this work were: rabbit anti-β-Gal (Cappel), anti-Rab7 (abcam), anti-Spectrin (DSHB) antibodies. Fluorochrome-conjugated secondary antibodies were purchased from Invitrogen, Molecular Probes. Images were obtained with a Zeiss AxioImager Z1 Microscope equipped with a Zeiss Apotome.

Acknowledgements

We thank Gisela Helbig and Silvia Tannebaum for excellent technical support. We thank Christine Tibbe for assistance in some experiments. We thank A. K. Basler, A. Martinez-Arias, S. Eaton, H. Bellen, F.-B. Gao, M. Gonzalez-Gaitan, Trudi Schüpach, M. Takemura and A. Nakamura for supplying fly stocks and reagents used in this work. The Bloomington Stock Center, VDRC and the Developmental Studies Hybridoma Bank also supplied fly stocks and reagents.

Competing interests

The authors declare no competing or financial interests.

Author contributions

K.S.M. and M.S. designed and performed experiments; T.K. designed and supervised experiments and wrote the manuscript.

Funding

The work was funded by the Deutsche Forschungsgemeinschaft (DFG) [SFB 590 and KL1028-1].

Supplementary material

Supplementary material available online at
<http://dev.biologists.org/lookup/suppl/doi:10.1242/dev.112961/-/DC1>

References

- Basel-Vanagaite, L., Attia, R., Yahav, M., Ferland, R. J., Anteki, L., Walsh, C. A., Olender, T., Straussberg, R., Magal, N., Taub, E. et al. (2006). The CC2D1A, a member of a new gene family with C2 domains, is involved in autosomal recessive non-syndromic mental retardation. *J. Med. Genet.* **43**, 203-210.
- Bastock, R. and St Johnston, D. (2008). Drosophila oogenesis. *Curr. Biol.* **18**, R1082-R1087.
- Bray, S. J. (2006). Notch signalling: a simple pathway becomes complex. *Nat. Rev. Mol. Cell Biol.* **7**, 678-689.
- Casanueva, M. O. and Ferguson, E. L. (2004). Germline stem cell number in the Drosophila ovary is regulated by redundant mechanisms that control Dpp signaling. *Development* **131**, 1881-1890.
- Childress, J. L., Acar, M., Tao, C. and Halder, G. (2006). Lethal giant discs, a novel C2-domain protein, restricts notch activation during endocytosis. *Curr. Biol.* **16**, 2228-2233.
- Couturier, L., Trylinski, M., Mazouni, K., Darnet, L. and Schweisguth, F. (2014). A fluorescent tagging approach in Drosophila reveals late endosomal trafficking of Notch and Sanpodo. *J. Cell Biol.* **207**, 351-363.
- de Navascués, J., Perdigoto, C. N., Bian, Y., Schneider, M. H., Bardin, A. J., Martínez-Arias, A. and Simons, B. D. (2012). Drosophila midgut homeostasis involves neutral competition between symmetrically dividing intestinal stem cells. *EMBO J.* **31**, 2473-2485.
- Gallagher, C. M. and Knoblich, J. A. (2006). The conserved c2 domain protein lethal (2) giant discs regulates protein trafficking in Drosophila. *Dev. Cell* **11**, 641-653.
- Harris, R. E. and Ashe, H. L. (2011). Cease and desist: modulating short-range Dpp signalling in the stem-cell niche. *EMBO Rep.* **12**, 519-526.
- Hu, Y., Ye, Y. and Fortini, M. (2002). Nicastrin is required for gamma-secretase cleavage of the Drosophila Notch receptor. *Dev. Cell* **2**, 69-78.
- Huotari, J. and Helenius, A. (2011). Endosome maturation. *EMBO J.* **30**, 3481-3500.
- Hurley, J. H. (2010). The ESCRT complexes. *Crit. Rev. Biochem. Mol. Biol.* **45**, 463-487.
- Jaekel, R. and Klein, T. (2006). The Drosophila Notch inhibitor and tumor suppressor gene lethal (2) giant discs encodes a conserved regulator of endosomal trafficking. *Dev. Cell* **11**, 655-669.
- Jékely, G. and Rørth, P. (2003). Hrs mediates downregulation of multiple signalling receptors in Drosophila. *EMBO Rep.* **4**, 1163-1168.
- Kai, T. and Spradling, A. (2003). An empty Drosophila stem cell niche reactivates the proliferation of ectopic cells. *Proc. Natl. Acad. Sci. USA* **100**, 4633-4638.
- Lloyd, T. E., Atkinson, R., Wu, M. N., Zhou, Y., Pennetta, G. and Bellen, H. J. (2002). Hrs regulates endosome membrane invagination and tyrosine kinase receptor signaling in Drosophila. *Cell* **108**, 261-269.
- Marois, E., Mahmoud, A. and Eaton, S. (2006). The endocytic pathway and formation of the Wingless morphogen gradient. *Development* **133**, 307-317.
- Martinelli, N., Hartlieb, B., Usami, Y., Sabin, C., Dordor, A., Miguet, N., Avilov, S. V., Ribeiro, E. A., Jr, Göttlinger, H. and Weissenhorn, W. (2012). CC2D1A is a regulator of ESCRT-III CHMP4B. *J. Mol. Biol.* **419**, 75-88.
- Micchelli, C. A., Rulifson, E. J. and Blair, S. S. (1997). The function and regulation of cut expression on the wing margin of Drosophila: Notch, Wingless and a dominant negative role for Delta and Serrate. *Development* **124**, 1485-1495.
- Narbonne-Reveau, K., Besse, F., Lamour-Isnard, C., Busson, D. and Pret, A.-M. (2006). fused regulates germline cyst mitosis and differentiation during Drosophila oogenesis. *Mech. Dev.* **123**, 197-209.
- Ninov, N., Menezes-Cabral, S., Prat-Rojo, C., Manjón, C., Weiss, A., Pyrowolakis, G., Affolter, M. and Martín-Blanco, E. (2010). Dpp signaling directs cell motility and invasiveness during epithelial morphogenesis. *Curr. Biol.* **20**, 513-520.
- Nüsslein-Volhard, C. and Wieschaus, E. (1980). Mutations affecting segment number and polarity in Drosophila. *Nature* **287**, 795-801.
- Parks, A. L., Klueg, K. M., Stout, J. R. and Muskavitch, M. A. T. (2000). Ligand endocytosis drives receptor dissociation and activation in the Notch pathway. *Development* **127**, 1373-1385.
- Rees, J. S., Lowe, N., Armean, I. M., Roote, J., Johnson, G., Drummond, E., Spriggs, H., Ryder, E., Russell, S., St Johnston, D. et al. (2011a). In vivo analysis of proteomes and interactomes using Parallel Affinity Capture (iPAC) coupled to mass spectrometry. *Mol. Cell. Proteomics* **10**, pM110.002386.
- Schneider, M., Troost, T., Grawe, F., Martínez-Arias, A. and Klein, T. (2013). Activation of Notch in lgd mutant cells requires the fusion of late endosomes with the lysosome. *J. Cell Sci.* **126**, 645-656.
- Sun, J. and Deng, W.-M. (2007). Hindsight mediates the role of notch in suppressing hedgehog signaling and cell proliferation. *Dev. Cell* **12**, 431-442.
- Sweeney, N. T., Brennan, J. E., Jan, Y. N. and Gao, F.-B. (2006). The coiled-coil protein shrub controls neuronal morphogenesis in Drosophila. *Curr. Biol.* **16**, 1006-1011.
- Szabad, J., Jursnich, V. A. and Bryant, P. J. (1991). Requirement for cell-proliferation control genes in Drosophila oogenesis. *Genetics* **127**, 525-533.
- Terracoli, R. and Lengyel, J. (1994). The thick veins gene of Drosophila is required for dorsoventral polarity of the embryo. *Genetics* **138**, 165-178.
- Thacker, S. A., Bonnette, P. C. and Duronio, R. J. (2003). The contribution of E2F-regulated transcription to Drosophila PCNA gene function. *Curr. Biol.* **13**, 53-58.
- Thompson, B. J., Mathieu, J., Sung, H.-H., Loeser, E., Rørth, P. and Cohen, S. M. (2005). Tumor suppressor properties of the ESCRT-II complex component Vps25 in Drosophila. *Dev. Cell* **9**, 711-720.
- Togon, E., Wollscheid, N., Cortese, K., Tacchetti, C. and Vaccari, T. (2014). ESCRT-0 is not required for ectopic Notch activation and tumor suppression in Drosophila. *PLoS ONE* **9**, e93987.
- Troost, T., Jaekel, S., Ohlenhard, N. and Klein, T. (2012). The tumour suppressor Lethal (2) giant discs is required for the function of the ESCRT-III component Shrub/CHMP4. *J. Cell Sci.* **125**, 763-776.
- Usami, Y., Popov, S., Weiss, E. R., Vriesema-Magnuson, C., Calistri, A. and Göttlinger, H. G. (2012). Regulation of CHMP4/ESCRT-III function in human immunodeficiency virus type 1 budding by CC2D1A. *J. Virol.* **86**, 3746-3756.
- Vaccari, T. and Bilder, D. (2005). The Drosophila tumor suppressor vps25 prevents nonautonomous overproliferation by regulating notch trafficking. *Dev. Cell* **9**, 687-698.
- Vaccari, T., Rusten, T. E., Menut, L., Nezis, I. P., Brech, A., Stenmark, H. and Bilder, D. (2009). Comparative analysis of ESCRT-I, ESCRT-II and ESCRT-III function in Drosophila by efficient isolation of ESCRT mutants. *J. Cell Sci.* **122**, 2413-2423.
- Xia, L., Jia, S., Huang, S., Wang, H., Zhu, Y., Mu, Y., Kan, L., Zheng, W., Wu, D., Li, X. et al. (2010). The fused/smurf complex controls the fate of Drosophila germline stem cells by generating a gradient BMP response. *Cell* **143**, 978-990.
- Xie, T. and Spradling, A. C. (2000). A niche maintaining germ line stem cells in the drosophila ovary. *Science* **290**, 328-330.
- Xu, T. and Rubin, G. M. (1993). Analysis of genetic mosaics in developing and adult Drosophila tissues. *Development* **117**, 1223-1237.
- Yousefian, J., Troost, T., Grawe, F., Sasamura, T., Fortini, M. and Klein, T. (2013). Dmon1 controls recruitment of Rab7 to maturing endosomes in Drosophila. *J. Cell Sci.* **126**, 1583-1594.
- Zender, L., Xue, W., Zuber, J., Semighini, C. P., Krasnitz, A., Ma, B., Zender, P., Kubicka, S., Luk, J. M., Schirmacher, P. et al. (2008). An oncogenomics-based in vivo RNAi screen identifies tumor suppressors in liver cancer. *Cell* **135**, 852-864.

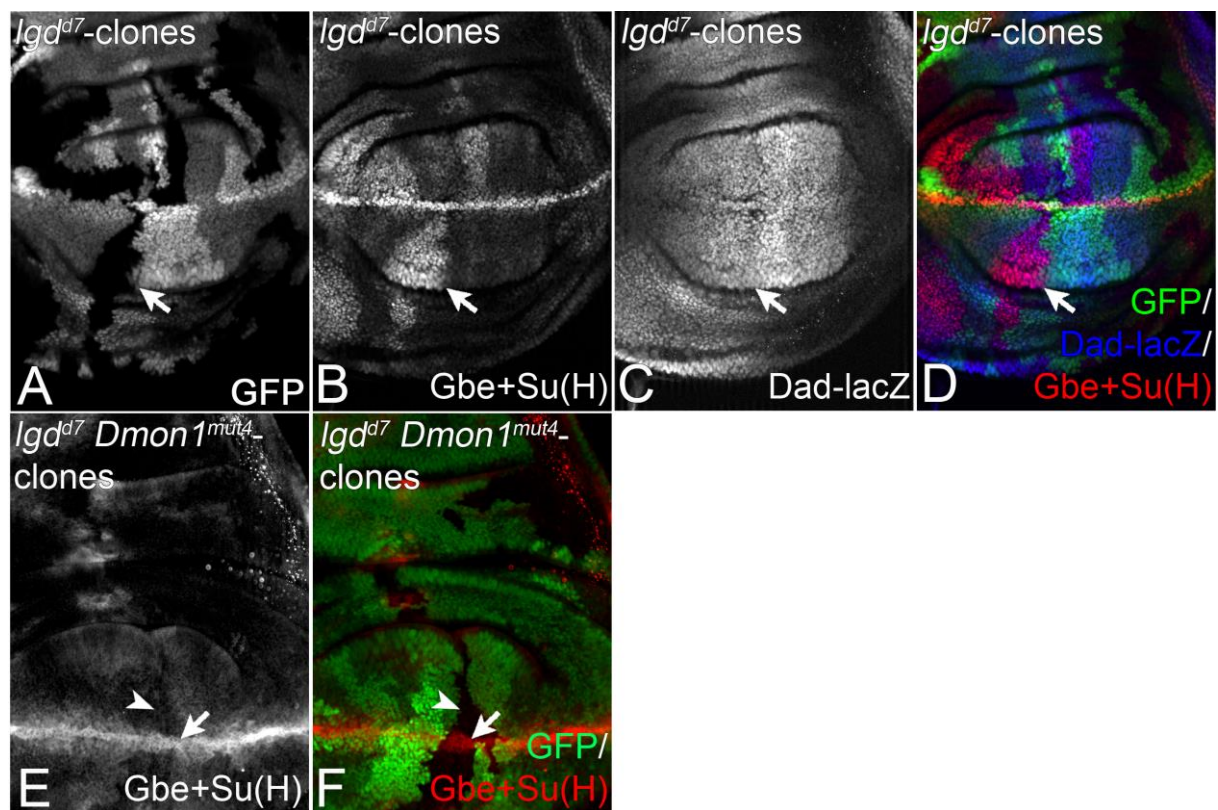


Fig. S1. Analysis of the activity of the Dpp and Notch pathways in *lgd* mutant and *lgd Dmon1* double mutant cell clones of the wing imaginal disc. (A-D) Loss of *lgd* function in the wing imaginal discs results in activation of the Notch but not the Dpp pathway. The clones are labelled by absence of GFP. While the Notch activity marker is upregulated in *lgd* mutant clones, the expression of *dad-lacZ* is not affected. The arrow highlights one of the clones. (E, F) the loss of function of *Dmon1* in *lgd* cells results in a suppression of the ectopic activation of the Notch pathway. The arrow point to a *lgd* mutant clone that cross the dorsoventral (D/V) boundary of the wing anlage. While the ligand dependent activation of Gbe+Su(H) along the D/V boundary is not affected (arrow) no ectopic activation of the Notch activity reporter can be observed in the area of the *lgd Dmon1* clone, away from the boundary (arrowhead). This is in contrast to the loss of function of *lgd* shown in (B, arrow).

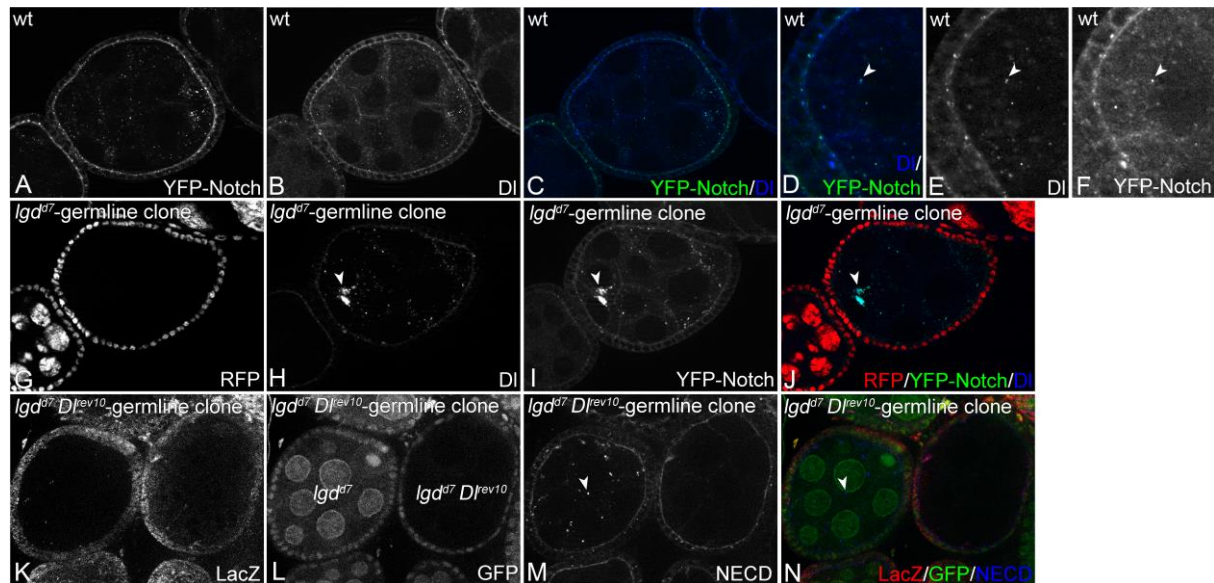


Fig. S2. DI signalling from GCs to FCs causes the accumulation of the NECD in GCs.

(A-F) Wildtype egg chamber. YFP-Notch and DI co-localise in endosomes of the GCs. The arrowhead points to one of the DI and YFP-Notch. (G-J) Colocalisation of YFP-N and DI in the enlarged endosomes of *lgd* mutant GCs (arrowhead). (K-N) Generation of *Dl lgd* double mutant GCs. The clones are generated in *hsFlp; lgd^{d7} FRT 40A/ arm. lacZ FRT40A; D^{rev10} FRT82B/ Ub.GFP FRT 82B* flies. (K) Two egg chambers where *lgd* is lost, indicated by the loss of lacZ staining. (L) The absence of GFP in the right chamber indicate that this chamber has also lost the function of *Dl* in its GCs. (M) The left *lgd* mutant GCs contain the NECD (arrowhead). In contrast, NECD is absent in the right *Dl lgd* double mutant GCs. This indicates that the accumulation of NECD in GCs is dependent of the presence of DI. (N) merge of the single channels shown in (K-M).

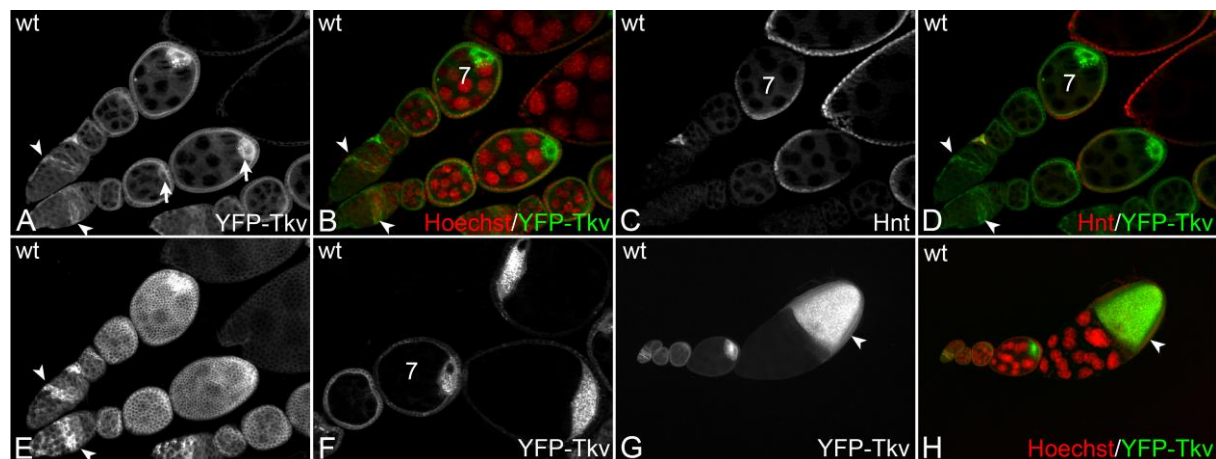


Fig. S3. Expression of YFP-Tkv during oogenesis. (A-E) Comparison of expression of YFP-Tkv with that of Hnt. (E) The ovarioles shown in (A-D) at the plane of the follicle epithelium. YFP-Tkv is expressed in all cells of the germarium at different levels during normal oogenesis. Surprisingly, the expression in the GSCs and cystoblasts is low compared to the surrounding cells. Expression peaks in the mitotic cyst stage 2B (arrowheads in A, B, D and E). Tkv-GFP continues to be expressed at high levels in early egg chambers up to stage 6/7 in FCs and GCs. During stage 6/7 it overlaps with the expression of Hnt. Moreover, is accumulates in the oocyte from stage 3 onwards (arrows in A). (F-H) After stage 7, expression declines to low levels in in FCs and GCs with the exception of the oocyte, which maintains high levels of Tkv-GFP throughout the rest of development. From stage 10 onwards the levels of Tkv-YFP increases again in FCs that surround the oocyte (G, H, arrowhead).

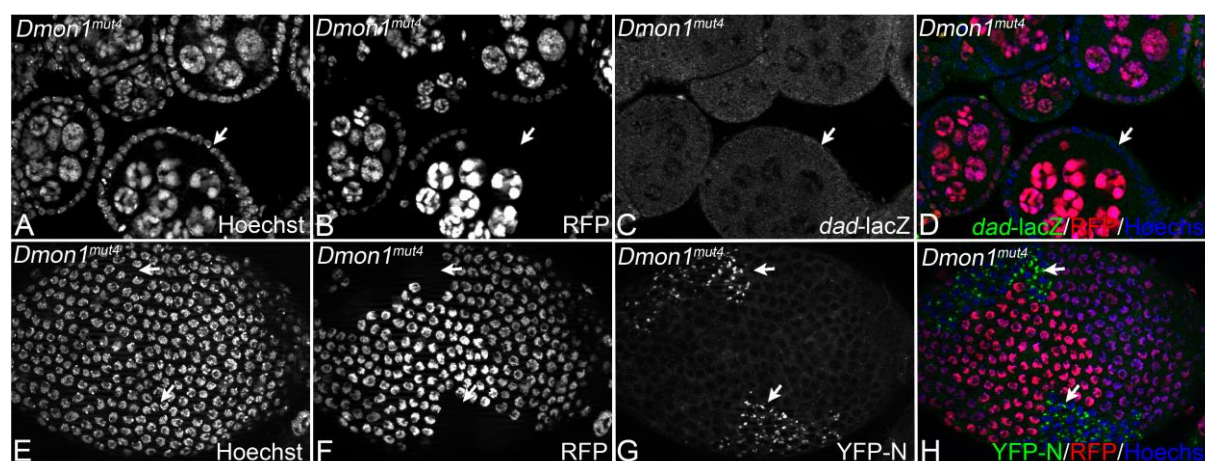
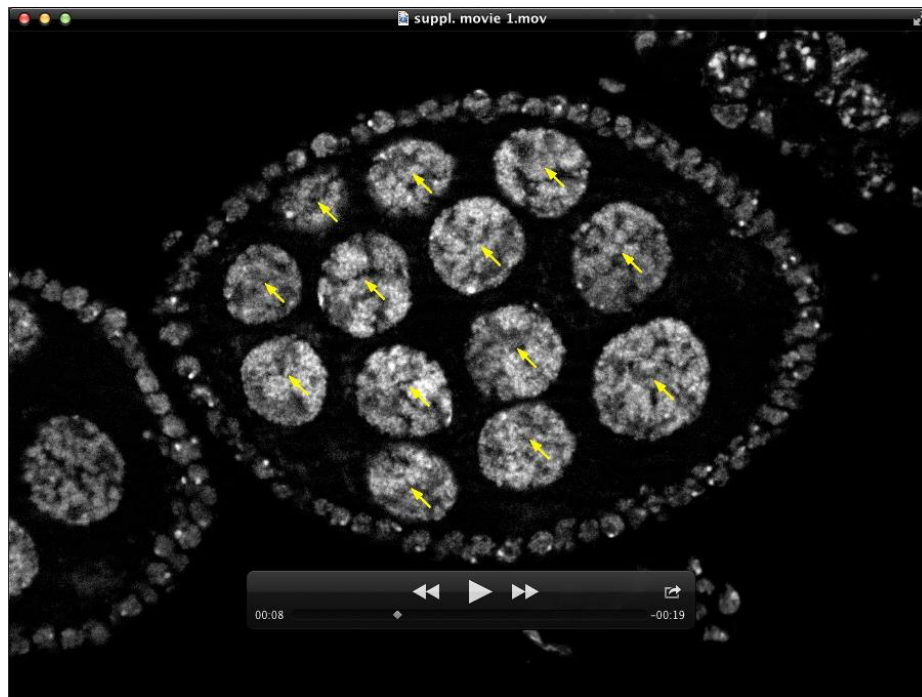


Fig. S4. *Dmon1* clones in FCs. The arrows point to the clones. (A-D) Expression of *dad-lacZ* is unaffected by loss of *Dmon1* function. (E-H) The mutant cells accumulate Notch in enlarged endosomes.



Movie 1. Movie through an *lgd* mutant EC with 32 GCs. The GCs are highlighted by the yellow arrows.